Numerical Investigation of Hydrogen Plumes and Comparison with Experiments in STG

Mathis Rosenhauer, Klaus Plähn[1] and Klaus Hannemann

Institute for Fluid Mechanics, German Aerospace Center
Bunsenstraße 10, 37073 Göttingen, Germany

Abstract. Hydrogen plumes gained much interest from the fact that H_2 is an important reaction product of a hydrazine thruster. H_2 shows strong and temperature dependant rotational relaxation which quickly leads to nonequilibrium between translational and rotational temperature in expanding flows. In a hybrid calculation of the whole flowfield, both methods (Navier-Stokes and DSMC) must model rotational relaxation consistently. Jeans' equation was used for Navier-Stokes, and for DSMC the Borgnakke-Larsen model with constant and with energy-dependent relaxation probability was used. The comparison with free molecule probe measurements of hydrogen plumes in the DLR High Vacuum Facility STG provides insight into the accuracy of the numerical models.

EXPERIMENTAL SET UP

Hydrogen is an important species in the exhaust plume of a hydrazine thruster. To prepare tests with real hydrazine thrusters, simulated plumes of pure hydrogen have been studied in the DLR High Vacuum Facility STG [1] (see fig. 1). The very high vacuum ($< 10^{-5}$ mbar) provided by the STG facility during thruster operation enables measurements with a free molecule pressure probe with negligible background disturbances throughout the whole flowfield. Because of the low boiling point of H_2, the cryo-pump which surrounds the expansion room has to be operated with liquid Helium.
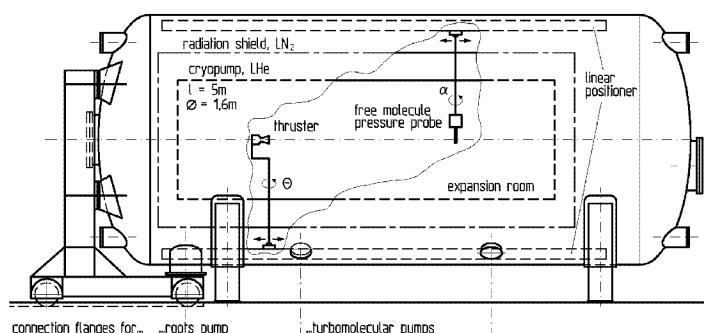

FIGURE 1. Cross section of the STG vacuum chamber with cold walls, thruster, probe and linear positioners.

The conical 0.5 N nozzle and the free molecule pressure probe can be rotated and the probe can also be moved in radial direction from the nozzle. Angular profiles of number flux were obtained by rotating the nozzle and radial profiles at different angles by moving the probe. The slit of the probe could have different orientations relative to the nozzle, but here the probe was always directly facing the nozzle. Stagnation pressure was held at

---

[1] now with WABCO Fahrzeugbremsen, Hannover

Report Documentation Page

Report Date	Report Type	Dates Covered (from... to)
09JUL2000	N/A	-

Title and Subtitle	**Contract Number**
Numerical Investigation of Hydrogen Plumes and Comparison with Experiments in STG	**Grant Number**
	Program Element Number

Author(s)	**Project Number**
	Task Number
	Work Unit Number

Performing Organization Name(s) and Address(es)	**Performing Organization Report Number**
Institute for Fluid Mechanics, German Aerospace Center Bunsenstrafie 10, 37073 Gottingen, Germany	

Sponsoring/Monitoring Agency Name(s) and Address(es)	**Sponsor/Monitor's Acronym(s)**
AOARD Unit 45002 APO AP 96337-5002	**Sponsor/Monitor's Report Number(s)**

Distribution/Availability Statement
Approved for public release, distribution unlimited

Supplementary Notes
Papers from Rarefied Gas Dynamics (RGD) 22nd International Symposium held in Sydney, Australia on 9-14 July 2000. See also ADM001341 for whole conference on cd-rom.

Abstract

Subject Terms

Report Classification	**Classification of this page**
unclassified	unclassified

Classification of Abstract	**Limitation of Abstract**
unclassified	UU

Number of Pages
6

$p_0 = 0.95$ bar and temperature $T_0 = 300K$. These conditions yield a nozzle exit Reynolds number of $R_E = 800$. The nozzle wall had a temperature of $300K$.

CONTINUUM METHOD

The hydrogen flow inside the nozzle was calculated with the DLR Navier-Stokes solver CEVCATS, a block-structured 3D upwind finite-volume code developed at DLR [2,3]. CEVCATS uses a hybrid AUSM - van Leer method for flux calculation and multigrid methods with residual averaging and local time-stepping to accelerate convergence to steady state. The modelling of the rotational energy relaxation was implemented following Jeans' equation [4],

$$\frac{d\epsilon_r}{dt} = \frac{\epsilon_r^*(t) - \epsilon_r(t)}{\tau_r}, \quad \tau_r = Z_r \tau_c,$$ (1)

where $\epsilon_r^*(t)$ is the instantaneous equilibrium rotational energy which is $\epsilon_r^*(t) = \epsilon_r(\infty) = kT_t$ in the isothermal limit, τ_c is the instantaneous collision time. The rotational collision number Z_r is either constant or a function of the translational temperature T. The temperature and viscosity coefficient ω dependant Z_r is modelled as in the paper of Boyd [5] where good agreement with experimental data cited by Lambert [6] was shown:

$$Z_r = 10480/T^\omega.,$$ (2)

INTERFACING OF THE TWO METHODS

Parts of the boundary layer inside the nozzle and the flowfield outside the nozzle where the assumptions for the Navier-Stokes equations cease to be valid have to be calculated with DSMC. The exact location of this interface is determined by a parameter characterizing the deviation of the distribution function f from a Maxwell distribution [7,8]. A parameter which characterizes the breakdown of continuum is the maximum of the viscous-stress tensor $\tau_{i,j}$ and the heat flux vector q_i:

$$B = max(|\tau_{i,j}|, |q_i|).$$ (3)

The interface location was choosen such that this parameter didn't exceed 0.1. Figure 2 shows B along the interface which was choosen as a straight line from the nozzle axis to the nozzle wall.
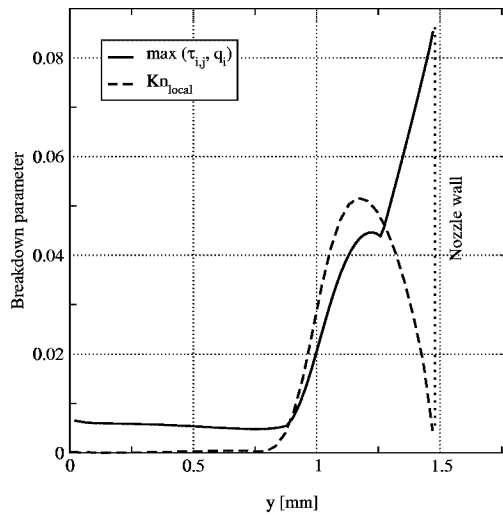

FIGURE 2. Continuum breakdown parameters along the method interface

B stays very low in the core flow but increases rapidly in the boundary layer because of the high viscous stress. Towards the nozzle wall, the temperature gradient and therefore the heat flux becomes dominant. As a reference, the local Knudsen number $Kn_{local} = \frac{\lambda}{\rho} \left| \frac{d\rho}{dy} \right|$ [7] is also plotted. Kn_{local} shows the same increase in the boundary layer but doesn't predict the nonequilibrium conditions near the nozzle wall due to the strong temperature gradient.

DSMC CALCULATION

The DSMC part of the flowfield was computed with the MONACO [9] code. The Natural-Sample-Size method by Baganoff and McDonald [10] is used as collision sampling technique. Collisions are simulated by the Variable Hard Sphere (VHS) and the Larsen–Borgnakke model [11]. A simple diffuse reflection model with full thermal accommodation handles gas–surface interaction. The code runs on different parallel architectures like Hitachi SR8000 and Sun Sparc MP.

The unstructured grid [12] was automatically adapted to the local mean free path, resulting in a grid size of 92000 cells. The flowfield was simulated with 7.7 million particles and one calculation took 90 h of computing time on one node of a Hitachi SR8000.

The inflow conditions for the DSMC part are given by the flow conditions of the Navier-Stokes solution at the interface. Here the flow is clearly not equilibrium any more, so the inflowing particles have to be generated from a Chapman-Enskog distribution. An acceptance-rejection random velocity generator for the Chapman-Enskog distribution as proposed by Garcia and Alder [13] is used.

Fig. 3 shows the number density as given by the Navier-Stokes solution and the number density at the interface, sampled from the first row of DSMC cells. The inflowing particles were generated from a Maxwell distribution and from the Chapman-Enskog distribution. While the densities agree very well in the core flow where the condition is near equilibrium, the particles generated from a Maxwell distribution lead to a much lower density near the nozzle wall than those generated from a Chapman-Enskog distribution which reproduce the density of the Navier-Stokes solution. This clearly shows that for this case, inflowing particles should be generated from a Chapman-Enskog distribution to model the inflow conditions correctly.
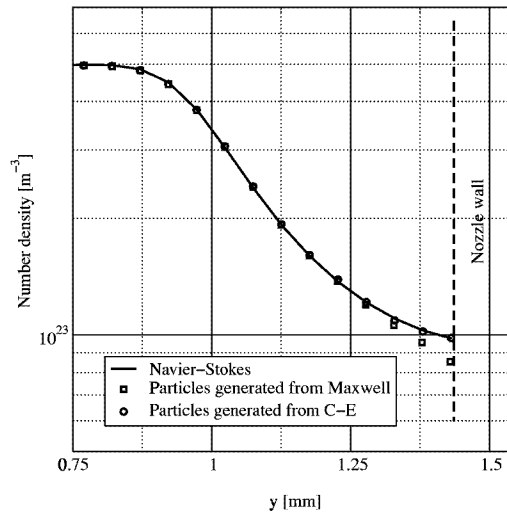

FIGURE 3. Number densities at the interface as given by the Navier-Stokes solution and sampled from the first row of DSMC cells.

It can be shown as in a paper by Boyd et al. [5] that an energy-dependant form of the probability of rotational energy exchange Φ_r reduces to (2) when integrated over the equilibrium distribution function,

$$\Phi_r = \frac{1}{10480} \frac{\Gamma(\zeta + 5/2 - \omega)}{\Gamma(\zeta + 5/2)} \left(\frac{E_c}{k}\right)^{\omega},$$

(4)

where E_c is the total collision energy, k is the Boltzmann constant and ζ is the number of degrees of freedom participating in the energy exchange process. Due to the difference between the probability of rotational energy exchange in DSMC and the macroscopic relaxation rate, some additional adjustments have to be made [5,14].

RESULTS

Figure 4a,b shows Navier-Stokes and DSMC calculations of translational and rotational temperature with temperature-dependant relaxation probablility in the vicinity of the nozzle.
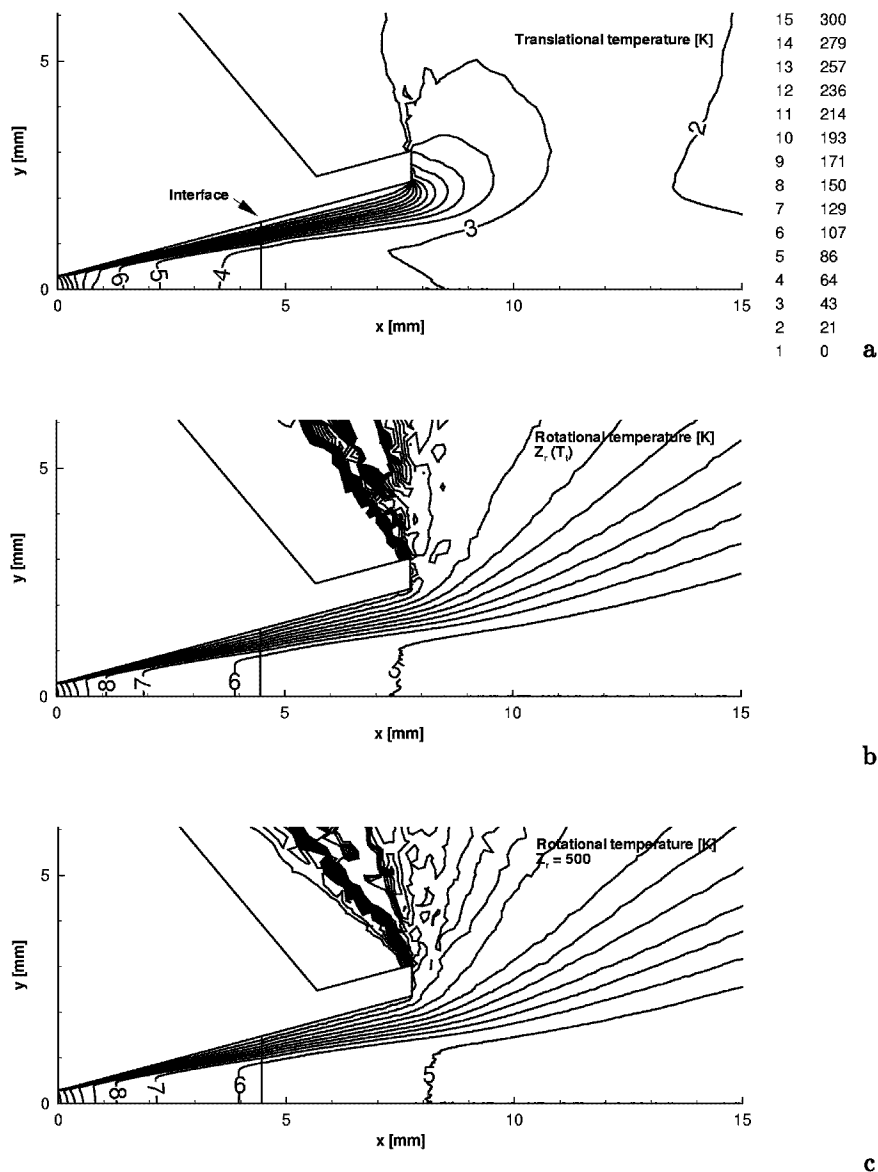

FIGURE 4. Navier-Stokes/DSMC calculation of a 0.5 N conical nozzle flow with $Re_E = 800$, testgas H_2. Contours of translational (a) and rotational temperature with temperature dependant (b) and constant (c) rotational collision number are shown.

Starting near the nozzle throat, the rotational temperature quickly departs from the translational temperature as expected for hydrogen. Figure 4c shows the rotational temperature calculated with constant $Z_r = 500$. Compared to 4b, the relaxation is faster near the nozzle throat and slower after the nozzle exit. Although the number of simulated molecules was too low in the backflow region to produce reliable rotational temperatures, the number density in this region indicates that for constant Z_r, more molecules are scattered at higher angles into the backflow due to the delayed transfer of rotational energy into the translational modes.

The comparison between measured and calculated number flux on radial and angular profiles is shown in figure 5. The total number flux, obtained by integrating the angular profiles over a sphere, shows good agreement between measurements and calculation. However, the plume shape as shown in the angular profile is predicted less slender by the calculation than the measurements indicate. This leads to a lower calculated number flux near the axis and somewhat higher flux for higher angles. The asymmetry in the measured plume comes from the influence of the high density measurements near the axis on the later measurements at larger negative angles due to incomplete outgassing. The radial profiles show the same overprediction of the calculation at higher angles. For the 90^0 case, the measurements show no decrease in number flux for higher radial distances which again indicates incomplete outgassing of the probe.
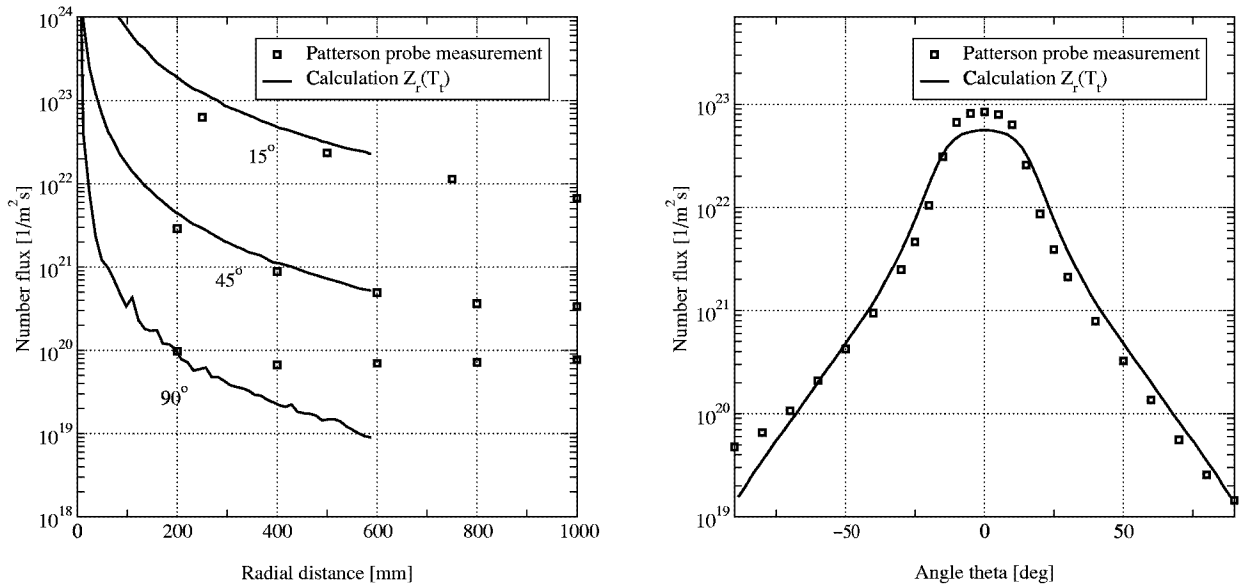

FIGURE 5. Patterson probe measuremens and calculations of H_2 number flux on radial and angular profiles.

Variation of the model parameters for rotational relaxation showed no significant influence, when compared with the number flux measurements in the available angular range. To decide on these details, direct measurements of the rotational temperature would give more insight. One reason for the differences in the plume shape may be the nozzle wall temperature which is only known at one point in the middle of the nozzle wall from the experiments. In the calculations, the nozzle wall was assumed to have a constant temperature which may not reflect the actual temperature distribution.

CONCLUSIONS

The hydrogen flowfield of a 0.5 N thruster nozzle was calculated with a decoupled hybrid Navier-Stokes – DSMC method. Consistent models for the relaxation of rotational temperature were implemented in both flow solvers with temperature-dependant and constant rotational relaxation number Z_r. To decide on the model and its parameters, comparison with measurements of rotational temperature are needed because the effect on the number flux, for which experimental data are already available, is too small. Experimental results of T_{rot}, density and velocity measurements with REMPI (Resonance Enhanced Multi Photon Ionisazion) for hydrogen will be available in the near future so the calculations can be compared with an additional independant set of

measurements. It was shown that it is important to generate particles which enter the DSMC region from a Chapman-Enskog distribution because of the starting deviation from equilibrium in the Navier-Stokes solution. The calculations reproduced the total number flux found by integrating the patterson probe measurements. The plume shape was in quite good agreement with the measurements but the calculations predicted lower number flux on the axis and slightly increased number flux in the off-axis regions.

REFERENCES

1. K. Plähn *Experimentelle Untersuchung und Modellierung von Abgasstrahlen aus Kleintriebwerken in der Kryo-Vakuum-Anlage STG* DLR-Forschungsbericht 1999-39, 1999.
2. N. Kroll, R. Radespiel, C.-C. Rossow. Accurate and efficient flow solvers for 3D applications on structured meshes, in "Computational Fluid Dynamics". *VKI-LS 1994-05, Von Karman Institute for Fluid Dynamics, Rhode-Saint-Genèse*, Belgium, 1994
3. S. Brueck, R. Radespiel, J.M.A. Longo. Comparison of nonequilibrium flows past a simplified Space-Shuttle configuration. *AIAA 97-0275, 35th Aerospace Sciences Meeting & Exhibit, January 6-10* Reno, NV, 1997
4. I. J. Wysong and D. C. Wadsworth. Assessment of direct simulation Monte Carlo phenomenological rotational relaxation models. *Phys. Fluids,* 10(11):2983–2994 (1998).
5. I. D. Boyd, D. R. Beattie and M. A. Cappelli. Numerical and experimental investigations of low-density supersonic jets of hydrogen. *J. Fluid Mech.,* 280:41–67 (1994)
6. J. D. Lambert *Vibrational and Rotational Relaxation in Gases* Oxford University Press, 1977.
7. I. D. Boyd, G. Chen, and G. V. Candler. Predicting failure of the continuum fluid equations in transitional hypersonic flows. *Phys. Fluids,* 7(1):210–219 (1995).
8. J. D. George and I. D. Boyd. Simulation of Nozzle Plume Flows Using a Combined CFD-DSMC Approach. *AIAA 99-3454, 33rd AIAA Thermophysics Conference* Norfolk, VA, June 1999.
9. S. Dietrich and I. D. Boyd. Scalar and parallel optimized implementation of the Direct Simulation Monte Carlo method. *J. Comp. Phys.,* 126(2):328–342 (July 1996)
10. D. Baganoff and J.D. McDonald. A collision selection rule for a particle simulation suited to vector computers. *Phys. Fluids A,* 2(7), 1990
11. G. A. Bird. *Molecular Gas Dynamics and the Direct Simulation of Gas Flows.* Oxford University Press, 1994.
12. J. R. Shewchuk. Triangle: Engineering a 2D quality mesh generator and delaunay triangulator. *First Workshop on Applied Computational Geometry, Philadelphia, Pennsylvania, ACM* pp. 124-133, May 1996
13. A. L. Garcia and B. J. Alder. Generation of the Chapman-Enskog distribution. *J. Comp. Phys.,* 140:66–70 (1998)
14. B. L. Haas, D. B. Hash, G. A. Bird, F. E. Lumpkin and H. A. Hassan. Rates of thermal relaxation in direct simulation monte carlo methods. *Phys. Fluids,* 6(6):2191–2201 (June 1994).